THE RESISTANCE OF METALLIC SANDWICH BEAMS WITH LATTICE CORES TO UNDER-WATER SHOCK LOADING

Norman A. Fleck

Cambridge University Engineering Dept., Trumpington St., Cambridge, CB2 1PZ, UK

ABSTRACT

Analytical models for the dynamic response of sandwich beams to an under-water shock are developed. The relative performance of the clamped beams is sensitive to the choice of the core topology of the beams. It is found that lattice cores with high through-thickness and longitudinal strength outperform metallic foam cores. It is concluded that sandwich panels have high potential as lightweight structures capable of mitigating shock.

1 INTRODUCTION

A major consideration in the design of military vehicles (such as ships) is their resistance to under-water shock loading. Lightweight metallic sandwich structures, with solid faces and lattice cores, show promise as shock resistant structures over the traditional monolithic plate design. In this paper, the shock resistance of the clamped sandwich beam is explored, see Fig. 1. Whilst it is appreciated that the precise dynamic response of practical designs is different from that explored here for beams, the qualitative details will be similar, and major simplifications arise from the fact that simple analytical formulae can be derived for the beam. The relative compressive strength of a range of lattice cores is explored in order to select the optimal core for shock application.

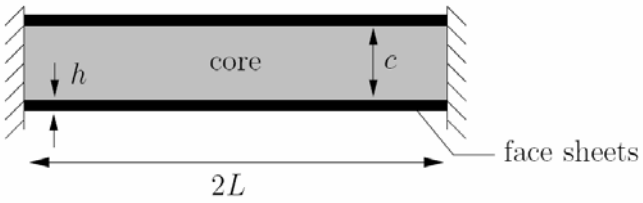

Fig. 1 Geometry of the clamped sandwich beam

1.1 Review of the characteristics of a water or air shock

The main characteristics of a shock wave from an under-water explosion are well established due to a combination of detailed large scale experiments and modelling over the past 60 years, see for example Ashby et al.[1] and Smith and Hetherington[2]. The under-water detonation of a high explosive charge converts the solid explosive material into gaseous reaction products at pressures on the order of GPa and on a time scale of microseconds. A spherical shock wave propagates into the surrounding water at approximately sonic speed. Consider the response of a representative fluid element at a radial distance r from the explosion. Upon arrival of the primary shock wave, the pressure rises to a peak value p_o on the order of 10-100 MPa almost instantaneously. Subsequently, the pressure decreases with time t at a nearly exponential rate, with a time constant θ on the order of 0.1ms, and is given by

$$p = p_o e^{-t/\theta} \tag{1}$$

The magnitude of the shock wave peak pressure and decay constant depend upon the mass and type

of explosive material and the distance r. Secondary shock waves have much smaller peak pressures, and are usually much less damaging than the primary shock to a structure in the vicinity of the explosion. A similar shock wave propagates in air due to the detonation of a high explosive. The primary shock wave travels at near sonic speed, with an exponential pressure-time history at any fixed location from the explosive. The time constant θ for the pulse is similar in magnitude to that in water, but the peak pressure is an order of magnitude lower.

The main objective of this paper is to develop analytical formulae for characterizing the structural response of lattice core sandwich beam subjected to shock loading in water or in air. First, the dynamic structural response of a clamped sandwich beam is analysed. Next, performance charts for a wide range of sandwich core topologies are constructed for water shock, with the monolithic beam taken as the reference case. Finally, these performance charts are used to determine the optimal geometry to maximize shock resistance for a given mass of sandwich beam.

2 ANALYTICAL MODEL FOR THE STRUCTURAL RESPONSE OF A CLAMPED SANDWICH BEAM TO SHOCK LOADING

The dynamic response is split into a sequence of 3 stages: stage I is the 1D fluid-structure interaction problem during the shock event, and results in a uniform velocity being imposed on the front face sheet; stage II involves core crush, during which the velocities of the faces and core equalise by momentum transfer; and stage III is the retardation phase during which the beam is brought to rest by plastic bending and stretching. This analysis is used to calculate the transverse displacement of selected sandwich beams as a function of the magnitude of shock loading. The justification for splitting the analysis into 3 distinct stages is the observation that the time-periods for the 3 phases differ significantly: 0.1 ms for the primary shock, 0.4 ms for the period for core crush and 25 ms for the structural response.

Stage I: 1D fluid structure interaction model

Consider the simplified but conservative idealisation of a plane wave impinging normally and uniformly upon an infinite sandwich plate. The timescale of the shock is sufficiently brief for the front face of a sandwich panel to behave as a rigid free-standing plate of mass per unit area m_f. Taylor[3] has analysed this problem; he considered an incoming wave in an elastic fluid of density ρ_w, travelling with a constant velocity c_w. The free standing plate is accelerated by the shock and emits a tensile wave back into the water until cavitation occurs. The net impulse conveyed to the front face is

$$I_{\text{trans}} = \varsigma I_o \tag{2}$$

where the knockdown factor is $\varsigma \equiv \psi^{-\psi/(\psi-1)}$ in terms of $\psi \equiv \rho_w c_w \theta / m_f$, and the maximum achievable impulse I_o is

$$I_o = \int_o^\infty 2 p_o e^{-t/\theta} dt = 2 p_o \theta \tag{3}$$

(The maximum impulse I_o is only realised for the case of a stationary rigid front face.) The front face is accelerated to a velocity $v_o = I_{trans} / m_f$ by the primary shock wave while the core and back face of the sandwich beam remain stationary; the core compression is negligible.

It is instructive to substitute some typical values for air and water shocks in order to assess the

knock-down in transmitted impulse. Consider a water shock with $\rho_w = 1000$ kgm^{-3}, $c_w = 1400$ ms^{-1}, $\theta = 0.1$ ms, and $m_f = 78$ kgm^{-2}; this implies $I_{\text{trans}} / I_o \approx 0.267$. We conclude that a significant reduction in transferred impulse can be achieved by employing a light face sheet for the case of water shock; in contrast, for an air shock, the large jump in acoustic impedance between air and the solid face sheet implies that all practical designs of solid face sheet behave essentially as a fixed, rigid face with full transmission of the shock impulse. We anticipate that sandwich panels with light faces can be designed to ensure the reduced transmission of impulse from an incoming water shock wave.

Stage II: 1D model of core compression phase

The core is crushed by the advancing front face sheet, and consequently the front face sheet is decelerated by the core whilst the core and the rear face of the sandwich beam are accelerated. For simplicity, consider a one dimensional slice through the thickness of the sandwich beam and neglect the reduction in momentum due to the impulse provided by the supports. Detailed finite element calculations carried out by Qiu *et al.*[4] support this assertion. The core is treated as a rigid, ideally plastic crushable solid with a nominal crush strength σ_{nY} up to a nominal densification strain ε_D. After densification has been achieved, it is assumed that the core is rigid.

Overall considerations of energy and momentum conservation can be used to determine the final value of core compressive strain $\varepsilon_c \left(\leq \varepsilon_D\right)$ and the final common velocity v_f of faces and core at the end of the core crush stage. Momentum conservation during core crush dictates that

$$\left(2m_f + m_c\right) v_f = m_f v_o \tag{3}$$

where m_c is the mass of the core. The ratio of the energy lost U_{lost} in this phase to the initial kinetic energy of the front face sheet is

$$\frac{U_{\text{lost}}}{m_f v_o^2 / 2} = \frac{1+\overline{m}}{2+\overline{m}} \tag{4}$$

in terms of $\overline{m} \equiv m_c / m_f$. This loss in energy is dissipated by plastic dissipation in compressing the core, giving

$$U_{\text{lost}} = \sigma_{nY} \varepsilon_c c \tag{5}$$

where ε_c is the average compressive strain in the core. Combining the two above relations, the core compression strain is given by

$$\varepsilon_c = \frac{\varepsilon_D}{2} \frac{1+\overline{m}}{2+\overline{m}} \hat{I}^2 \tag{6}$$

in terms of the dimensionless impulse $\hat{I} \equiv I_{\text{trans}} / \sqrt{m_f c \sigma_{nY} \varepsilon_D}$. However, if U_{lost} is too high such that ε_c as given by (6) exceeds the densification strain ε_D, then ε_c is set to the value ε_D and additional dissipation mechanisms must occur for energy conservation. The above analysis neglects any such additional mechanisms.

Stage III: dynamic structural response of clamped sandwich beam

At the end of stage II the core and face sheets have a uniform velocity v_f as given by (4). The final stage of sandwich response comprises the dissipation of the kinetic energy acquired by the beam during stages I and II by a combination of beam bending and longitudinal stretching. The problem reduces to the classical one: what is the dynamic response of a clamped beam of length *2L* made from a rigid ideally-plastic material with mass per unit length *m* subjected to an initial uniform transverse velocity v_f? Here we summarise the approximate solution of Fleck and Deshpande[5] that

is valid in both the small and large displacement regimes: it reduces to the exact small displacement solution of Symmonds[6] for small v_f and is nearly equal to the approximate large deflection solution of Jones[7] for large v_f.

The face sheets are made from a rigid ideally plastic material of yield strength σ_{fY} and density ρ_f, while the core of density ρ_c has a normal compressive strength σ_{nY} and a longitudinal strength σ_{lY}. The plastic bending moment of the sandwich beam with the compressed core is given by

$$M_o = \sigma_{lY}\frac{(1-\varepsilon_c)c^2}{4} + \sigma_{fY}h[(1-\varepsilon_c)c + h] \tag{7}$$

while the plastic membrane force N_o is given by

$$N_o = 2\sigma_{fY}h + \sigma_{lY}c \tag{8}$$

Introduce the non-dimensional geometric variables of the sandwich beam

$$\bar{c} \equiv \frac{c}{L},\ \ \bar{h} \equiv \frac{h}{c},\ \ \hat{c} \equiv \bar{c}(1-\varepsilon_c), \text{and}\ \ \hat{h} \equiv \frac{\bar{h}}{(1-\varepsilon_c)} \tag{9}$$

and the non-dimensional core properties

$$\bar{\rho} \equiv \frac{\rho_c}{\rho_f},\ \ \bar{\sigma}_l \equiv \frac{\sigma_{lY}}{\sigma_{fY}},\ \ \text{and}\ \ \ \bar{\sigma}_n \equiv \frac{\sigma_{nY}}{\sigma_{fY}} \tag{10}$$

The non-dimensional measure of the shock impulse $\bar{I}$ is

$$\bar{I} \equiv \frac{I_o}{L\sqrt{\rho_f \sigma_{fY}}} \equiv \frac{\hat{I}\bar{c}\sqrt{\bar{\sigma}_n \varepsilon_D \bar{h}}}{\varsigma} \tag{11}$$

where ςI_o is the shock impulse transmitted to the structure by the fluid. In terms of these non-dimensional groups, the maximum deflection *w* of the back face of the sandwich beam is

$$\bar{w} \equiv \frac{w}{L} = \frac{\alpha_2}{2}\left[\sqrt{1 + \frac{8\bar{I}^2\varsigma^2\alpha_3}{3\alpha_1\alpha_3}} - 1\right] \tag{12}$$

where

$$\alpha_1 = \hat{c}^3\left[\left(1+2\hat{h}\right)^2 - 1 + \bar{\sigma}_l\bar{c}/\hat{c}\right]\left(1+2\hat{h}\right)\bar{c}\left(\bar{\rho} + 2\bar{h}\right)$$

$$\alpha_2 = \frac{\hat{c}\left[\left(1+2\hat{h}\right)^2 - 1 + \bar{\sigma}_l\bar{c}/\hat{c}\right]}{2\hat{h} + \bar{\sigma}_l\bar{c}/\hat{c}} \qquad \text{and} \qquad \alpha_3 = \hat{c}\left(1+2\hat{h}\right) \tag{13}$$

3 PREDICTIONS

The above analysis gives the deflection $\bar{w}$ and the core compression ε_c in the sandwich beam in terms of: (i) the shock impulse $\bar{I}$, and fluid-structure interaction parameter ψ; (ii) the beam geometry $\bar{c}$ and $\bar{h}$; and (iii) the core properties as given by the core relative density $\bar{\rho}$, its longitudinal tensile strength $\bar{\sigma}_l$, compressive strength $\bar{\sigma}_n$ and its densification strain ε_D.

3.1 Core topologies

Over the last decade, a number of new core topologies for sandwich beams have emerged. Here we consider the candidate core topologies shown in Fig. 2: pyramidal core, prismatic diamond core, corrugated core, metal foam, square honeycomb, hexagonal-honeycomb and an ideal core. The relevant mechanical properties of the cores (assumed to be made from an elastic, ideally-plastic

solid material with yield strain ε_Y) in terms of the normalised transverse compressive strength $\overline{\sigma}_n$ and longitudinal strength $\overline{\sigma}_l$ are listed in Table 1 as functions of the relative density $\overline{\rho}$ of the cores. The ideal core is 100 % efficient in carrying load in both the transverse and longitudinal directions, although it is unclear whether such a core is physically realisable. The compressive strength of a number of these cores has been measured recently for the case of 304 stainless steel, of yield strength 210 MPa. The measured strengths are compared in Fig. 3.

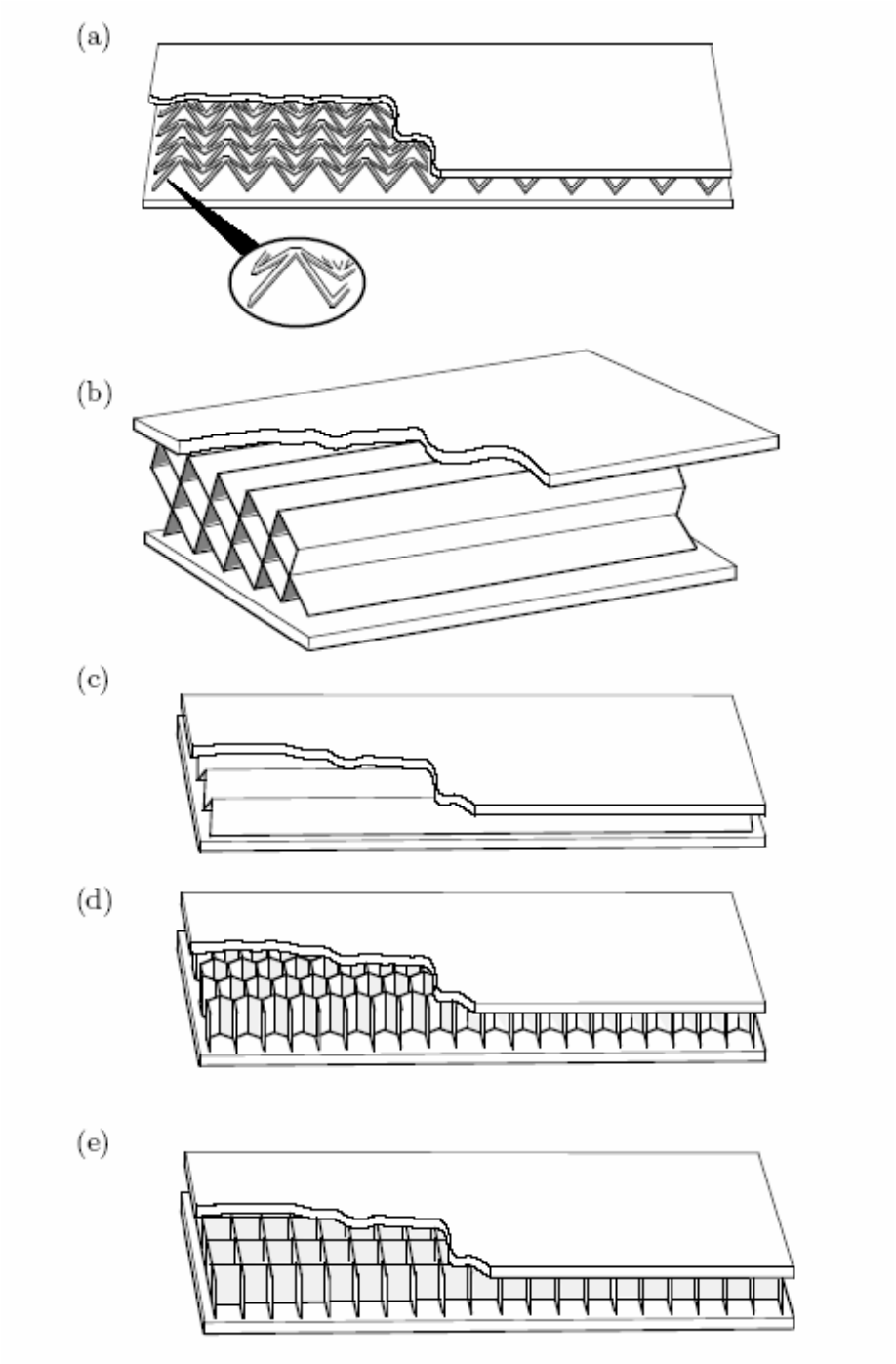

Fig. 2. Sketches of the sandwich core topologies. (a) pyramidal, (b) diamond-celled, (c) corrugated, (d) hexagonal honeycomb, and (e) square honeycomb.

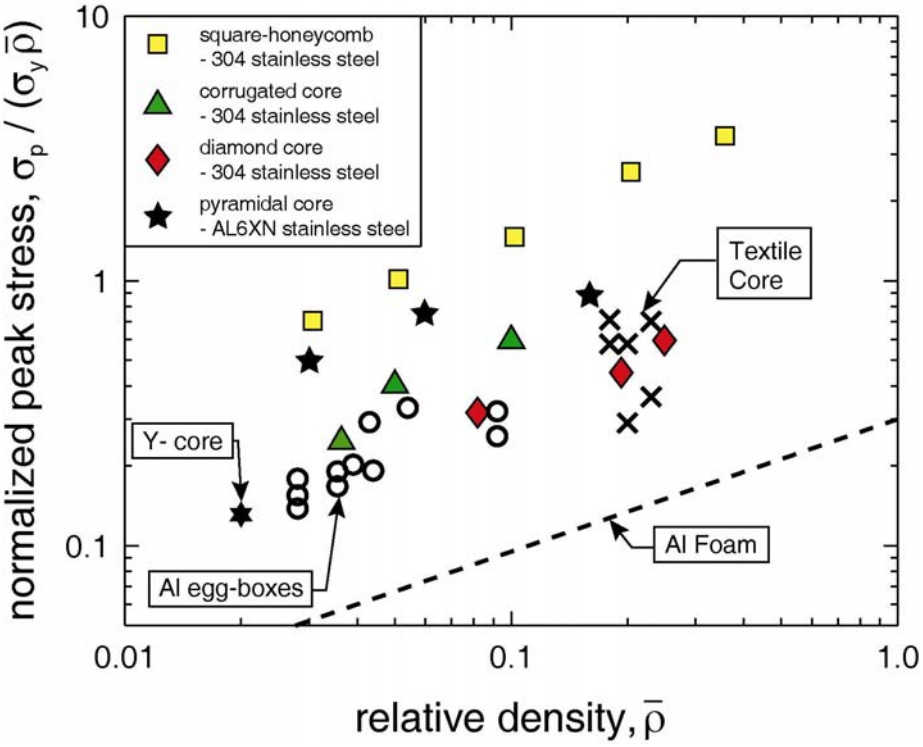

Fig. 3. Measured compressive strength of competing core topologies as a function of the core relative density $\overline{\rho}$.

Table 1: Transverse and longitudinal strengths of core topologies.

Core design	$\overline{\sigma}_n$	$\overline{\sigma}_l$
Pyramidal truss core	$0.5\overline{\rho}$ if $\overline{\rho} > \frac{96\sqrt{2}\varepsilon_Y}{\pi^2}$ $\frac{\pi^2}{96\sqrt{2}\varepsilon_Y}\overline{\rho}^2$ otherwise	0
Metal foam core	$0.3\overline{\rho}^{3/2}$	$0.3\overline{\rho}^{3/2}$
Hexagonal-honeycomb core	$\overline{\rho}$	0
Square-honeycomb core	$\overline{\rho}$	$0.5\overline{\rho}$
Prismatic diamond-celled or Corrugate core	$0.5\overline{\rho}$ if $\overline{\rho} > \frac{4\sqrt{3\varepsilon_Y}}{\pi}$ $\frac{\pi^2}{96\varepsilon_Y}\overline{\rho}^3$ otherwise	$\overline{\rho}$
Ideal core	$\overline{\rho}$	$\overline{\rho}$

4 PERFORMANCE CHARTS FOR WATER SHOCK RESISTANCE AND OPTIMAL DESIGN

The analysis detailed above is now used to investigate the relative response of monolithic and sandwich beams to shock loading. In a typical design, the length of the structural element is dictated by design constraints such as the bulkhead spacing, thus leaving the sandwich panel topology as free

design variables: the face sheet and core thickness, the type of core and its relative density. For a given material combination, beam length and allowable back face sheet deflection, what is the relation between the required sandwich geometry and the level of imposed shock impulse?

For the sandwich beam, introduce a fluid-structure interaction parameter $\overline{\psi}$

$$\overline{\psi} \equiv \psi \frac{h}{L} = \frac{\rho_w c_w \theta}{L} \tag{14}$$

which is closely related to the Taylor fluid-structure interaction parameter ψ but written in terms of the specified beam length. Thus, the impulse I_{trans} transmitted to the beam is given by (2) for a specified value of $\overline{\psi}$ and a known beam geometry h/L.

The shock response of clamped sandwich beams, comprising solid faces and the six types of cores*, will be analysed in this section. We restrict attention to cores made from the same solid material as the solid face sheets in order to reduce the number of independent non-dimensional groups by one. With the sandwich beam length and material combination specified, the design variables in the problem are the non-dimensional core thickness $\overline{c}$ and face sheet thickness $\overline{h}$.

Consider the representative case of a clamped sandwich beam with a pyramidal core $(\overline{\rho} = 0.1,\ \varepsilon_{\text{Y}} = 0.002,\ \varepsilon_D = 0.5)$, subjected to a water shock such that $\overline{\psi} = 5\times10^{-3}$ (representative of a $2L = 10$ m long steel beam subject to a shock with time constant $\theta = 0.12$ ms). Contours of imposed shock impulse are shown as a function of $\overline{c}$ and $\overline{h}$ for a specified deflection $\overline{w} = 0.1$ in Fig. 4.

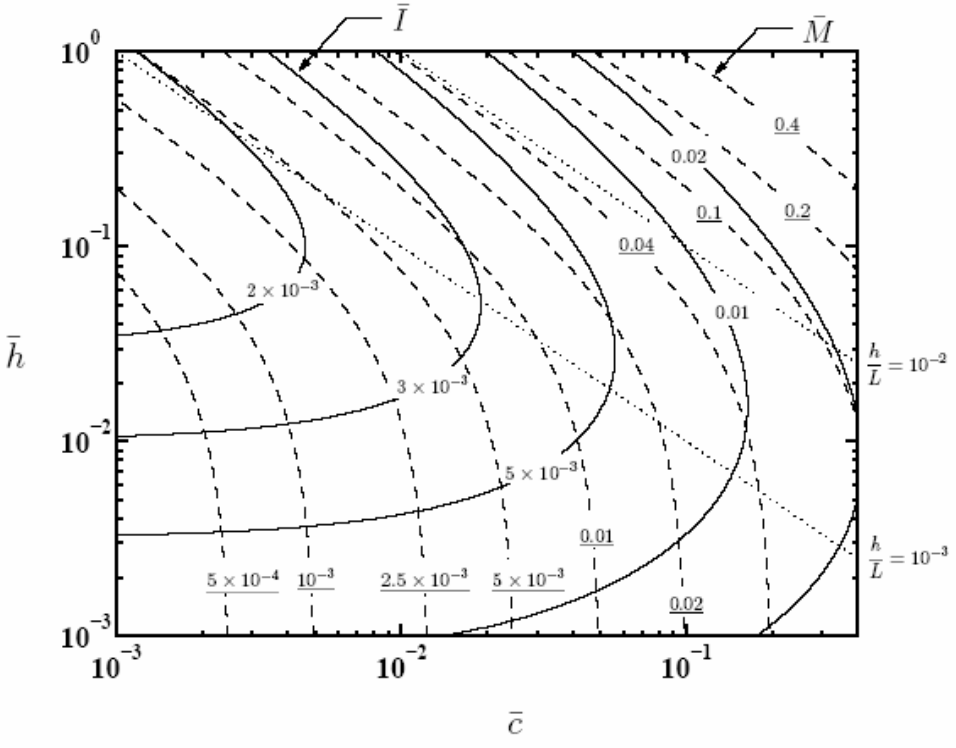

Fig. 4. Design chart for a sandwich beam, with a pyramidal core $(\overline{\rho} = 0.1, \varepsilon_Y = 0.002, \varepsilon_D = 0.5)$, subjected to a water blast. The beam deflection is $\overline{w} = 0.1$ and the fluid-structure interaction parameter is taken as $\overline{\psi}$ =5x10^{-3}. Contours of $\bar{I}$ and $\overline{M}$ are displayed. The dotted lines trace the paths of selected values of *h/L*.

* In the present analysis the corrugated and prismatic diamond core have an identical response

For the purposes of selecting sandwich beam geometries that maximise the shock impulse at a given mass *M*, subject to the constraint of a maximum allowable back face deflection $\overline{w}$, contours of non-dimensional mass $\overline{M} = M/\rho_f L^2$ have been added to Fig. 4. The geometries that maximise the shock impulse $\bar{I}$ at a given mass $\overline{M}$ lie on $\bar{h} \to 0$, at almost constant $\bar{c}$, implying that $h/L \to 0$. The physical interpretation is as follows. With decreasing face sheet thickness (or face sheet mass) the shock impulse transmitted to the structure reduces: the Taylor analysis gives $I_{\text{trans}} \to 0$ as $h \to 0$. This limit is practically unrealistic as a minimum face sheet thickness is required for other reasons, for example to withstand wave loading, quasi-static indentation by foreign objects such as rocks and other vessels and fragment capture in a shock event. Consequently, we add the additional constraint of a minimum normalised face sheet thickness h/L to the analysis. Contours of h/L in Fig. 4 represent limits on acceptable sandwich beam designs, with designs lying above these lines satisfying the constraint on h/L. Designs that maximise shock impulse for a given mass then lie along the lines of constant h/L.

The maximum shock impulse sustained by the sandwich beams with the six different topologies of the core ($\overline{\rho} = 0.1$, $\varepsilon_{\text{Y}} = 0.002$ and $\varepsilon_D = 0.5$ in all cases), subject to the constraints $h/L > 10^{-2}$ and the back face deflection $\overline{w} \le 0.1$ are plotted in Fig. 5 as a function of the non-dimensional mass $\overline{M}$ for the choice $\overline{\psi} = 5\times10^{-3}$. For comparison purposes, the shock impulse sustained by a monolithic beam subjected to the same constraints is also included in Fig. 5.

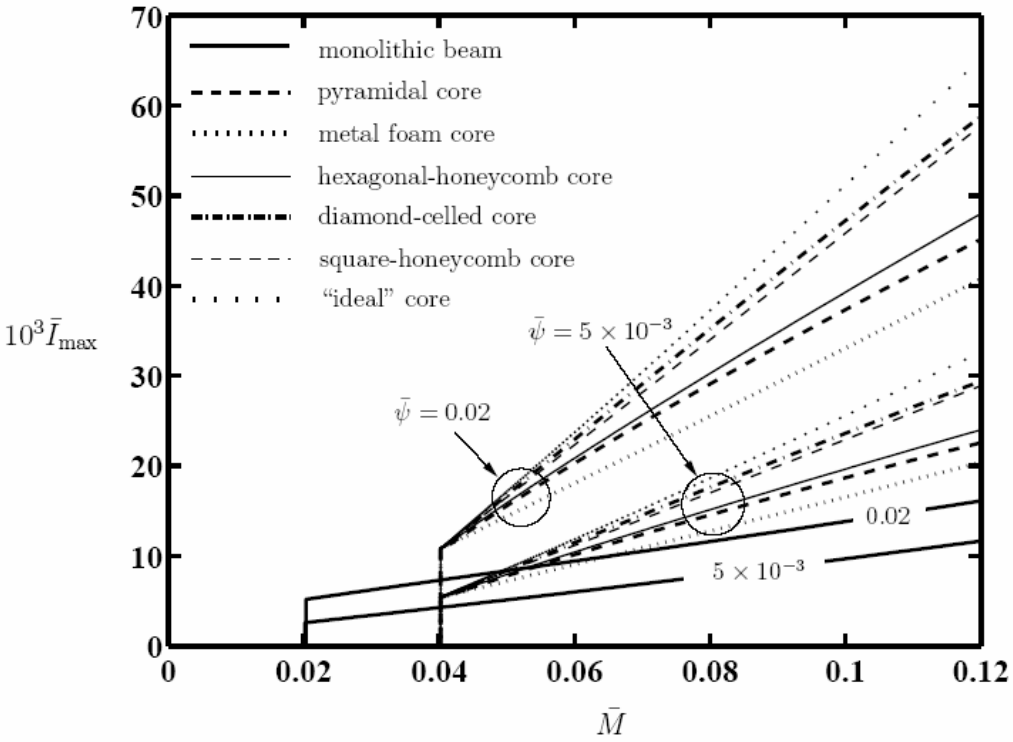

Fig. 5 A comparison of the maximum shock impulse sustained by monolithic beams and by optimal designs of sandwich beams, subjected to the constraints $\overline{w} \le 0.1$ and $h/L \ge 10^{-2}$. Results are presented for $\overline{\psi}$ =5x10^{-3} and 0.02. The core relative density is $\overline{\rho}$ =0.1, its yield strain is ε_Y =0.002 and the densification strain is ε_D =0.5.

It is evident that sandwich beams all perform considerably better than the monolithic beam. This is mainly due to the fact that the sandwich beams have a thin front face sheet which results in a small impulse transmitted into the structure whereas the relatively thick beams in monolithic design absorb a larger fraction of the shock impulse. A comparison of the various sandwich cores shows

that sandwich beams with a metal foam and pyramidal core almost attain the performance of the hexagonal-honeycomb core. However, the diamond-celled and square-honeycomb core beams, which have high strength in both the through-thickness and longitudinal directions, out-perform the other sandwich beams. The performance of the diamond-celled core approaches that of the ideal sandwich core. It is noted that $\overline{M}$ has minimum achievable values due to the constraint on the minimum value of h/L. With increasing values of the $\overline{\psi}$, the fraction of the shock impulse transmitted into the structure decreases and thus all the beams sustain higher shock. However, the relative performance of the various beam configurations remains unchanged.

5 CONCLUDING REMARKS

An approximate analytical methodology has been presented to predict the dynamic response of sandwich beams under-water shock loading. A number of approximations have been made to make the problem tractable to an analytical solution. Principally, these are (i) the 1D approximation of the shock event, (ii) separation of the stages of the response into three sequential phases, (iii) neglect of the support reaction during the shock event and during the core compression phases and (iv) a highly simplified core constitutive model wherein the core is assumed to behave as a ideally plastic locking solid. The effects of strain hardening and rate sensitivity of the solid material has also been neglected. Despite these approximations, the analysis has been shown to compare well with 3D FE calculations of Xue and Hutchinson[8]. Thus, the analysis presented here is not only adequate to explore trends and scaling relations but is also expected to suffice to make approximate predictions for the purposes of selecting core topologies and sandwich beam geometries. The non-dimensional formulae presented here bring out the stages of the response clearly and hence aid the interpretation of more accurate numerical calculations such as the recent dynamic finite element analysis.

The analysis has been used to construct performance charts for the response of both monolithic and sandwich beams subject to water borne shocks. An order of magnitude improvement in shock resistance is achieved by employing sandwich construction. This is mainly due to fluid-structure interaction: the reduced mass of the sandwich front face leads to a reduction in the impulse transmitted to the structure from the water. The diamond-celled core sandwich beam gives the best performance due to the longitudinal strength provided by the core.

ACKNOWLEDGEMENTS

The authors are grateful to ONR for their financial support through US-ONR IFO grant number N00014-03-1-0283.

REFERENCES

[1] M.F. Ashby, A.G. Evans, N.A. Fleck, L.J. Gibson, J.W. Hutchinson, and H.N.G. Wadley, *Metal Foams: A Design Guide*, Butterworth Heinemann, Boston, 2000.

[2] P.D. Smith and J.G. Hetherington, *Shock and Ballistic Loading of Structures*, Butterworth Heinemann, 1994.

[3] G.I. Taylor, 'The pressure and impulse of submarine explosion waves on plates', *The scientific papers of G I Taylor*, **Vol III**, pp287, 1941.

[4] X. Qiu, V.S. Deshpande and N.A. Fleck, 'Finite element analysis of the dynamic response of clamped sandwich beams subject to shock loading', *European Journal of Mechanics A/Solids*, **22**, pp801-814, 2003.

[5] N.A. Fleck, and V.S. Deshpande, 'The resistance of clamped sandwich beams to shock loading', *Journal of Applied Mechanics*, **71**, pp386-401, 2004.

[6] P.S. Symmonds, ‘Large plastic deformations of beams under shock type loading’, *Proceedings of the second US National Congress of Applied Mechanics*, pp505, 1954.
[7] N. Jones, ‘A theoretical study of the dynamic plastic behaviour of beams and plates with finite deflections’, *International Journal of Solids and Structures*, **7**, pp1007-1029, 1971.
[8] Z. Xue and J.W. Hutchinson, (2004). ‘A comparative study of shock-resistant metal sandwich plates’. To appear in *International Journal of Impact Engineering*.